Simulation of Boundary Layer Structure over the Indian Summer Monsoon Trough during the Passage of a Depression

K. V. J. POTTY

IBM India Research Laboratory, Indian Institute of Technology, New Delhi, India

U. C. MOHANTY

Centre for Atmospheric Sciences, Indian Institute of Technology, New Delhi, India

S. RAMAN

Department of Marine, Earth and Atmospheric Sciences, North Carolina State University, Raleigh, North Carolina

(Manuscript received 14 January 2000, in final form 11 October 2000)

ABSTRACT

The planetary boundary layer (PBL) structure over the Indian summer monsoon trough region has been simulated using a regional numerical model during the passage of a monsoon depression along the monsoon trough. Monin–Obukhov similarity theory for the surface layer coupled with turbulent kinetic energy closure scheme (1½-order closure) for the mixed layer is used for parameterizing the PBL in the model. The results show that the model is able to simulate the evolution and the structure of the monsoon trough boundary layer and its associated features. The main observed characteristic features of the monsoon trough, such as the southward tilt of the trough with height and warmer air mass toward the northern side of the trough line, are simulated well by the model. Numerical results also indicate that the dynamic and thermodynamic characteristics of the monsoon trough boundary layer are modified by the passage of monsoon depressions.

1. Introduction

The Indian summer monsoon trough is an elongated low pressure system that extends southeastward from Pakistan to Gangetic West Bengal, with southwesterly winds south of the trough line and easterlies to the north (Fig. 1). The presence of this semipermanent feature during the monsoon season (June–September) is considered as the equatorial trough of the summer period in the Indian longitudes. This trough extends aloft up to about 4 km and slopes southward with height. No other monsoon feature has such a control on monsoon activity over northern India as the monsoon trough (Rao 1976; Das 1986). The position of the trough changes day to day and has an important bearing on the summer monsoon rainfall over the Indian subcontinent. Once the trough line shifts toward the foothills of Himalayas, a "break" in the monsoon occurs. During the break in the monsoon period, rainfall decreases sharply over the subcontinent except over the foothills of the Himalayas. Marching of the trough toward the south invokes the formation of monsoon depressions over the north Bay of Bengal moving west to northwest across the country. Average rainfall is larger toward the south of the axis beause of the fact that the heavier rains occur in the southwest quadrant of the depressions. Major differences are noticed between the dynamic and thermal characteristics of the eastern and western ends of the trough. The western end of the trough line is somewhat diffused because of a weak wind field being associated with the heat low. The moisture content of the air is relatively low, and the boundary layer is capped with a stable layer above 1.5 km. The eastern end is well defined with a deep moist layer, which is warm and unstable and thermodynamically very active. Sikka and Narasimha (1995) have given a detailed description of the large-scale meteorological environment of the monsoon trough region. Because the monsoon rainfall is mainly due to convection, and the roots of deep convection lie near the surface, it will be of interest to study the evolution and the structure of the boundary layer over this convective low pressure (monsoon trough) region.

There have not been many modeling studies of planetary boundary layer (PBL) over the monsoon trough region. Holt and Sethu Raman (1988) compared the

Corresponding author address: Dr. K. V. Jayaraman Potty, IBM India Research Laboratory, Indian Institute of Technology, Hauz Khas, New Delhi 110 016, India.
E-mail: pjayaram@in.ibm.com

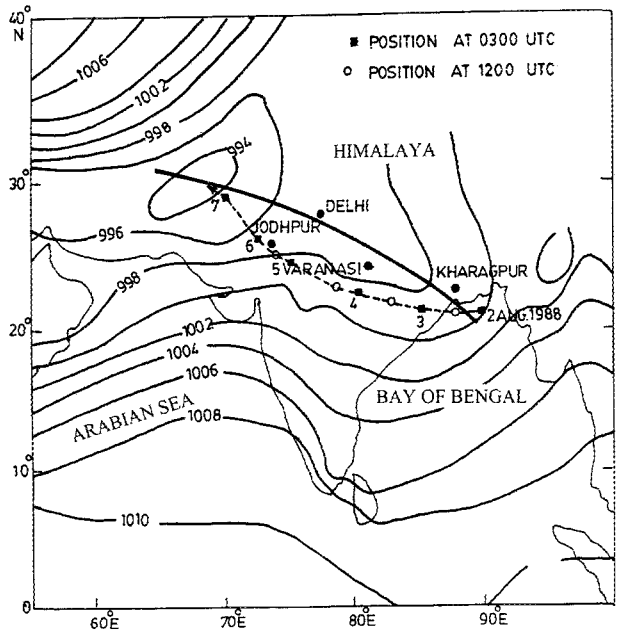

FIG. 1. Normal position of the monsoon trough (solid line), the track of the depression that formed during the period 3–5 Aug 1988 (dashed line), and the stations chosen for the simulation studies.

TABLE 1. A brief description of the model.

Domain	13.5–34.5°N, 66°–99°E
Independent variables	λ, Φ, σ, t
Prognostic variables	U, v, T, q, Ps
Diagnostic variables	ϕ, σ
Topography	Envelope (mean + 1 std dev)
Vertical grid system	16 levels in σ coordinates
Vertical levels of the model	0.05, 0.15, 0.25, 0.35, 0.45, 0.55, 0.65, 0.75, 0.82, 0.86, 0.90, 0.935, 0.960, 0.975, 0.987, and 0.997
Horizontal grid system	Arakawa C grid
Time integration scheme	Split-explicit time integration
Time step	150 s
Horizontal resolution	0.5° lat–long
Horizontal diffusion	Linear second order
Initialization	Nonlinear normal mode
Physical processes	Dry convective adjustment; Cumulus convection Kuo scheme with convective precipitation Large-scale stratified precipitation with RH >95% PBL; M–O similarity scheme for the surface layer, TKE ($E - e$) for the mixed layer

boundary layer structure over the oceanic region as simulated by a set of first-order and turbulent kinetic energy (TKE) closure schemes using a dataset from the 1979 Monsoon Experiment (MONEX-79). They used a one-dimensional boundary layer model for the study, and it showed that a 1½-order closure scheme performs better than first-order closure schemes. Alapaty et al. (1994) used a nested-grid regional model with a high vertical resolution in the atmospheric boundary layer to simulate various atmospheric processes during an active monsoon period. They found significant variation in boundary layer structure and associated processes over land as compared to oceans. Lykossov et al. (1991) simulated the temporal evolution of the boundary layer over the eastern region of the monsoon trough with a one-dimensional TKE–dissipation closure model using the Monsoon Trough Boundary Layer Experiment (MONTBLEX) pilot experiment dataset at Calcutta during 1988. Kusuma et al. (1991) have conducted sensitivity studies on atmospheric boundary layer for the monsoon trough region during the southwest monsoon season with one-dimensional TKE closure model and simulated the locally observed boundary layer structure with reasonable accuracy. Potty et al. (1997) studied the effect of three different boundary layer parameterization schemes in a regional model on the simulation of summer monsoon circulation and found that the Monin–Obukhov similarity theory for the surface layer and TKE closure (1½-order closure) scheme for the mixed layer constitute an appropriate combination for the parameterization of PBL over the Indian monsoon region. These results prompted us to simulate and examine the boundary layer structure and associated processes over the monsoon trough and adjoining oceanic region with the TKE closure scheme combined with the Monin–Obukhov (M–O) surface layer similarity theory for PBL parameterization. In this paper, the simulation results up to 48 h using a regional model pertaining to the evolution and structure of the PBL over the monsoon trough are presented. Initial conditions for integrating the model have been chosen in such a way that an already-formed monsoon depression was moving along the trough so that its impact on the PBL can be studied as well.

2. Model description

For the current study, a hydrostatic primitive equation model with a terrain-following coordinate system is used. The horizontal resolution of the model is 0.5° latitude–longitude, and, in the vertical, the model has 16 levels (8 levels up to 850 hPa) in sigma coordinates. The finite-difference form of the governing equations is of second-order accuracy in space. A split-explicit scheme (Madala 1978) is used for time integration. The details of the time-integration scheme employed in the model are described by Mohanty et al. (1990). The Arakawa-C grid (Arakawa and Lamb 1977) in the model has an energy-conserving staggered-grid system with uniform resolution in longitude and latitude. A sponge boundary condition of Perkey and Kreitzberg (1976) is employed for updating the lateral boundaries of the model, and a second-order diffusion equation is used in the model to handle the computational instabilities, which arise because of the subgrid scale processes. The physical processes included in the model are dry convective adjustment, large-scale precipitation, convective precipitation, and internal diffusion. Details of the mod-

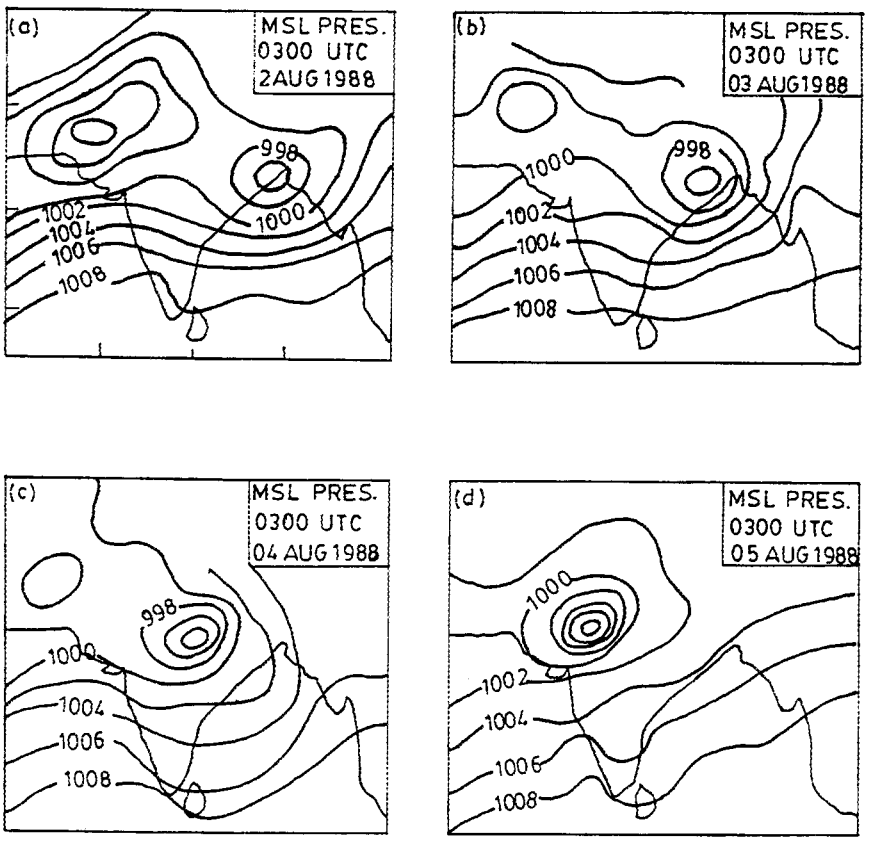

FIG. 2. Observed mean sea level pressure at 0300 UTC [0830 Indian standard time (IST)] for the dates (a) 2 Aug 1988, (b) 3 Aug 1988, (c) 4 Aug 1988, and (d) 5 Aug 1988 (source: India Meteorological Department).

el equations and numerics can be found in Madala et al. (1987). The horizontal domain of the model chosen for this study is from 13.5° to 34.5°N in the north–south direction and 66° to 99°E in the east–west direction so that the entire monsoon trough region falls in this domain. An overview of the model is given in Table 1.

3. Experimental details

The similarity (Monin and Yaglom 1971) approach has been used to parameterize the surface boundary layer in the model. Accordingly, the fluxes of momentum, heat, and moisture are given as

$$\frac{\partial u}{\partial z} = \frac{u_*}{kz}\Phi_m(Z/L), \tag{1}$$

$$\frac{\partial \theta}{\partial z} = \frac{\theta_*}{kz}\Phi_h(Z/L), \tag{2}$$

$$\frac{\partial q}{\partial z} = \frac{q_*}{kz}\Phi_h(Z/L). \tag{3}$$

Here, Φ_m and Φ_h are the nondimensional universal functions of the stability parameter Z/L (Businger et al. 1971). The scale length L is defined as

$$L = \frac{\overline{\theta_v} u_*^2}{kg\theta_*},$$

where g represents acceleration due to gravity, k is the von Kármán constant, u is the wind speed, z is the reference height, and θ_v is the virtual potential temperature. The terms u_*, θ_*, and q_* are defined by $u_*^2 = -\overline{u'w'}$, $u_*\theta_* = -\overline{w'\theta'}$, $u_*q_* = -\overline{w'q'}$, respectively. Prime indicates the perturbation from the mean. Businger et al. (1971) and a large number of researchers have explained how these universal functions are calculated and hence they are not explained here. Roughness length z_0 is considered as a function of terrain height over land and is calculated using (Krishnamurti et al. 1990)

$$z_0 = 0.15 + 0.2(236.8 + 18.42h)^2 \times 10^{-8}, \tag{4}$$

where h is the topography in meters. Over ocean, z_0 has been computed using Charnock's relation (Charnock 1955)

$$z_0 = 0.015u_*^2/g. \tag{5}$$

The ground wetness factor over the land for the computation of latent heat flux has been provided as a function of albedo and is given by (Kumar 1989)

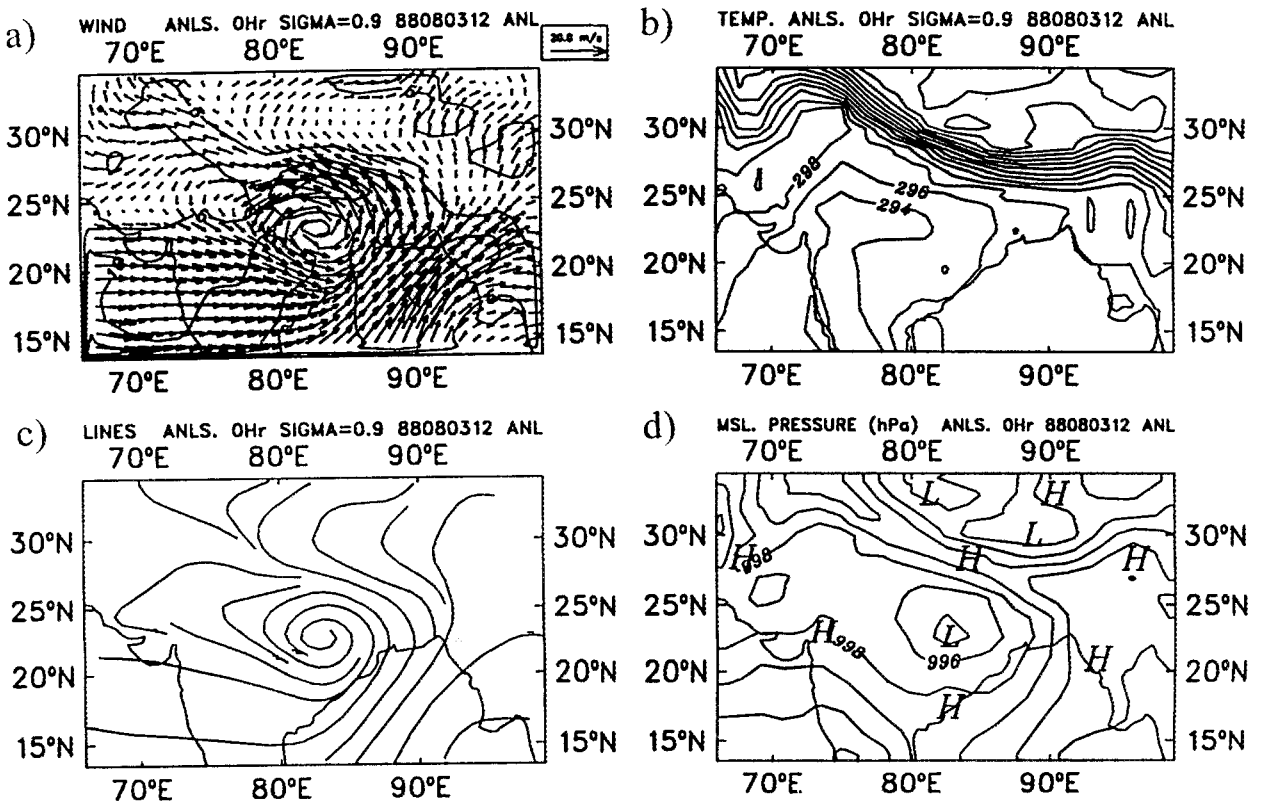

FIG. 3. Initial analysis of (3 Aug 1988 at 1200 UTC) (a) wind fields at 0.9 σ level, (b) temperature at 0.9 σ level, (c) streamlines at 0.9 σ level, and (d) mean sea level pressure.

$$\beta = 0.85\{1.0 - \exp[-200.0(0.31 - \text{Albedo})^2]\}. \quad (6)$$

Over the ocean surface, the value of β is taken as 1.0.

Above the surface layer, the PBL parameterization uses the TKE E–ϵ closure approach. Accordingly, the prognostic equation for TKE (E) is given as

$$\frac{\partial E}{\partial t} = -\overline{u'w'}\frac{\partial u}{\partial z} - \overline{v'w'}\frac{\partial v}{\partial z} + \frac{g}{\theta}\overline{w'\theta'} - \frac{\partial}{\partial z}(\overline{w'E'} + \overline{p'w'}/\rho) - \epsilon. \quad (7)$$

The first two terms on the right-hand side of the equation represent shear production, the third represents buoyancy production, the fourth represents turbulent transport, and the fifth is the dissipation of TKE. In the above equation, $\overline{u'w'}$ and $\overline{v'w'}$ are turbulence fluxes of momentum $\overline{w'\theta'}$ is the turbulence flux of heat, ρ is the density, and p is the fluctuating pressure.

The parameterization of individual terms such as shear production, buoyancy, turbulent transport, and so on, for TKE and its dissipation are summarized by Holt and Sethu Raman (1988) and are not explained here. However, the final form of the prognostic equation for TKE is given by

$$\frac{\partial E}{\partial t} = K_m\left[\left(\frac{\partial u}{\partial z}\right)^2 + \left(\frac{\partial v}{\partial z}\right)^2\right] + \frac{g}{\theta}K_h\frac{\partial \theta}{\partial z} + C_1\frac{\partial}{\partial z}\left(K_m\frac{\partial E}{\partial z}\right) - \epsilon. \quad (8)$$

In a similar manner, a prognostic equation for the dissipation of TKE (ϵ) is

$$\frac{\partial \epsilon}{\partial t} = C_3\frac{\epsilon}{E}\left(-\overline{u'w'}\frac{\partial u}{\partial z} - \overline{v'w'}\frac{\partial v}{\partial z} + \frac{g}{\theta}\overline{w'\theta'}\right) - C_4\frac{\epsilon^2}{E} + C_5\frac{\partial}{\partial z}\left(K_m\frac{\partial \epsilon}{\partial z}\right), \quad (9)$$

and its parameterized form is given by

$$\frac{\partial \epsilon}{\partial t} = C_3\frac{\epsilon}{E}\left\{K_m\left[\left(\frac{\partial u}{\partial z}\right)^2 + \left(\frac{\partial v}{\partial z}\right)^2\right] - \frac{g}{\theta}K_h\frac{\partial \theta}{\partial z}\right\} - C_4\frac{\epsilon^2}{E} + C_5\frac{\partial}{\partial z}\left(K_m\frac{\partial \epsilon}{\partial z}\right). \quad (10)$$

The relationship of eddy viscosity (K_m) and TKE in terms of dissipation is given by (Daly and Harlow 1970)

$$K_m = C_2 E^2/\epsilon. \quad (11)$$

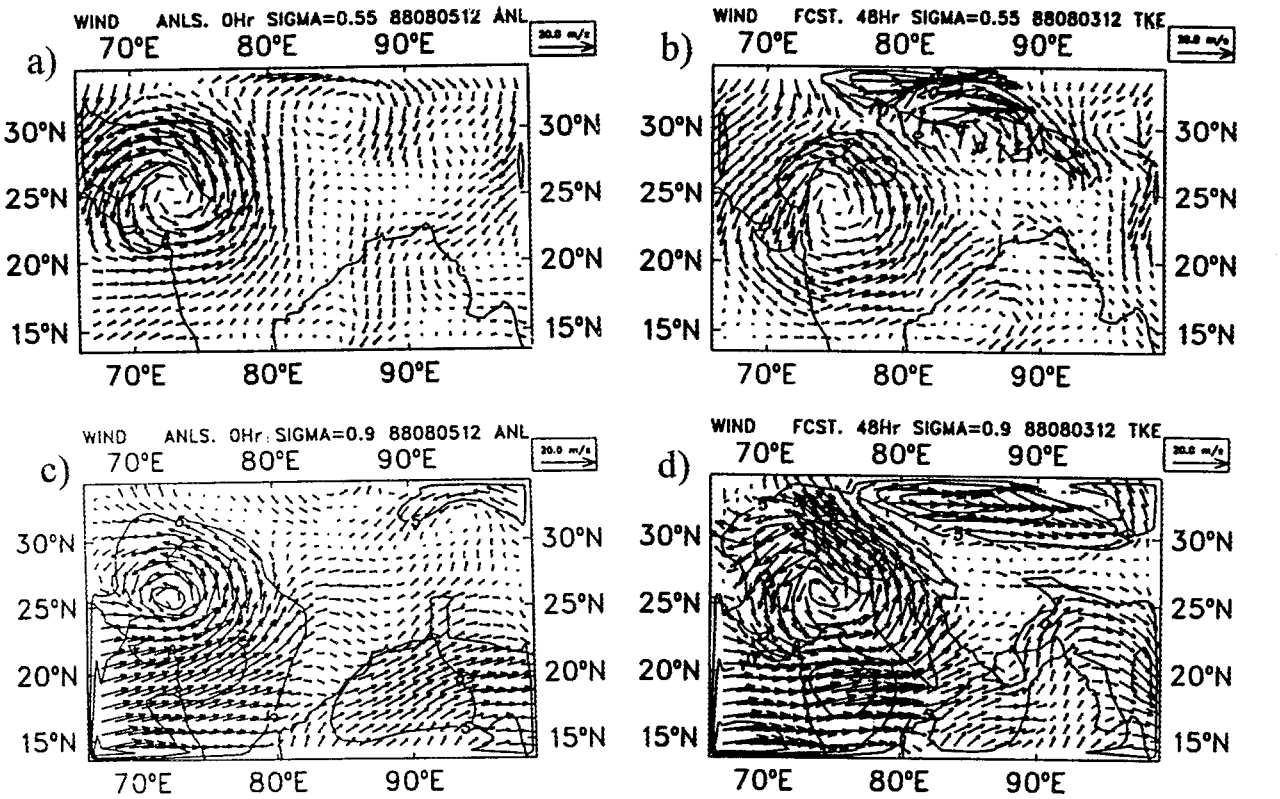

FIG. 4. Wind fields (a) analysis at 0.55 σ level on 5 Aug 1988 at 1200 UTC, (b) forecast (48 h) at 0.55 σ level, (c) analysis at 0.9 σ level on 5 Aug 1988, and (d) 48-h forecast at 0.9 σ level.

Holt and Sethu Raman (1988) studied the suitability of the values of constants (C_1 to C_5) used in the above equations of TKE and dissipation and found that the constants of Detering and Etling (1985) work well. Hence, for this study, the same set of constants has been used, and they are given by $C_1 = 1.35$, $C_2 = 0.026$, $C_3 = 1.13$, $C_4 = 1.9$, and $C_5 = 0.77$.

The solution of the TKE equation requires the specification of E in the surface layer (Mailhot and Benoit 1982), which should be a function of u_*, w_*, and Z/L. Based on Deardorff (1974) and Wyngaard (1975),

$$E = 3.75u_*^2 \qquad Z/L > 0,$$

$$E = 3.75u_*^2 + 0.2w_*^2 + (-Z/L)^{2/3}u_*^2 \qquad Z/L < 0,$$

$$\epsilon = u_*^3/kz,$$

where u_* is the frictional velocity and w_* is convective velocity, which is given by

$$w_* = [(g/T)h\overline{(w'T_v)_0'}]^{1/3},$$

where the subscript zero denotes near-surface values, and virtual temperature (T_v) flux is computed as

$$\overline{w'T_v'} = \overline{w'T'} + 0.61(T\overline{w'q'} + q\overline{w'T'}),$$

where h is the boundary layer height, which is computed from the previous iteration of TKE. The boundary layer height is given as the model level height at which TKE reduces to 0.05 $m^2\ s^{-2}$ or less. The upper boundary condition of the model is taken as $E = \epsilon = 0$.

Surface temperature over the water can be considered as a constant boundary condition for short-range forecast. However, the land surface temperature may vary considerably over a period of 12–24 h and hence its variation has to be computed for the lower boundary condition. The ground temperature has been computed using an energy balance equation following Lazic and Talenta (1990). Mean climatological sea surface temperature (SST) for the month of August is used for oceanic points.

The evolution of the boundary layer depends on the dynamical and thermodynamical effects at the locations considered. The land surface heats up at a much quicker rate than the oceanic region during the daytime, resulting in a large diurnal variation of surface temperature and other surface parameters. As the western sector of the monsoon trough is of dry convective regime, the evolution of the PBL and associated characteristic features are largely controlled by the thermal effects. On the other hand, the eastern sector of the monsoon trough is a moist convective region, and hence the transfer of sensible heat and its diurnal variation are considerably less. The local dynamical effects however play a significant role in the evolution of the PBL over the eastern side of the monsoon trough. MONTBLEX in 1990 was

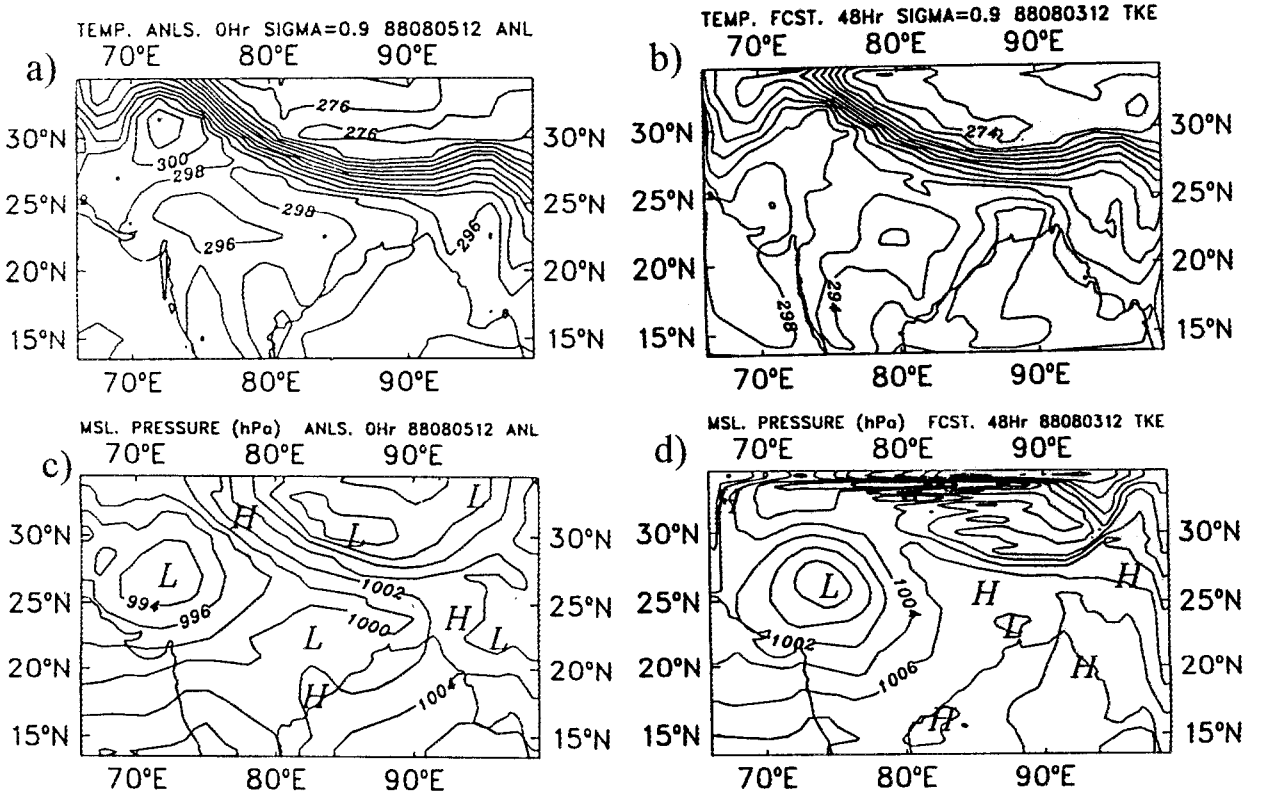

FIG. 5. (a) Analysis of temperature at 0.9 σ level on 5 Aug 1988 at 1200 UTC, (b) 48-h forecast of temperature at 0.9 σ level, (c) analysis of mean sea level pressure on 5 Aug 1988 at 1200 UTC, and (d) 48-h forecast of mean sea level pressure.

conducted to study the structure of the atmospheric boundary layer over the monsoon trough region (Goel and Srivastava 1990). Intensive observations were made at four stations (Jodhpur, Delhi, Varanasi, and Kharagpur) along the mean location of the monsoon trough during the period June to September 1990. Some of the results based on this experiment have already been published (Narasimha et al. 1997). Hence for the sake of comparison purposes, in this study, we also chose four grid points of the model close to the stations Jodhpur, Delhi, Varanasi, and Kharagpur along the monsoon trough to study the evolution of the PBL and the associated features over the Indian subcontinent (Fig. 1). One grid point each over the Arabian Sea and Bay of Bengal were also selected to study the PBL characteristics over the adjoining oceanic sectors.

The European Centre for Medium-Range Weather Forecasts operational analysis for 3–5 August 1988 at 1200 UTC are used as initial and boundary conditions for integrating the model. U.S. Navy 10′ × 10′ topography data and climatological SST for August have also been used for the model simulation.

4. Results and discussions

In this section, a brief discussion of the synoptic situation that prevailed over the monsoon trough region during the numerical experiment time (3–5 August 1988) and the initial analysis of selected fields are presented. Large-scale fields after 48 h of model integration are then discussed. Gridpoint results at selected stations and vertical cross sections pertaining to the boundary layer structure over the monsoon depression are depicted later.

a. Synoptic conditions

The summer monsoon of 1988 was a normal one, with the position of the monsoon trough mostly situated 2°–5° to the south of its normal position (Das et al. 1989). A depression developed over the north Bay of Bengal on 2 August 1988 and traveled across the country in a northwest direction up to the western part of Rajasthan on 7 August 1988, giving rise to copious rainfall across the region. The observed track of the depression during the period is also given in Fig. 1. The mean sea level pressure observed at 0300 UTC for the period 2–5 August 1988 are given in Fig. 2. Isobars in the figure show the presence of the depression and its movement. On 2 August at 0300 UTC, the low pressure area over the north Bay of Bengal coast developed into a depression and lay centered about 200 km southeast of Calcutta. On 3 August, it crossed the Calcutta coast and moved in a west-to-northwest direction. It crossed

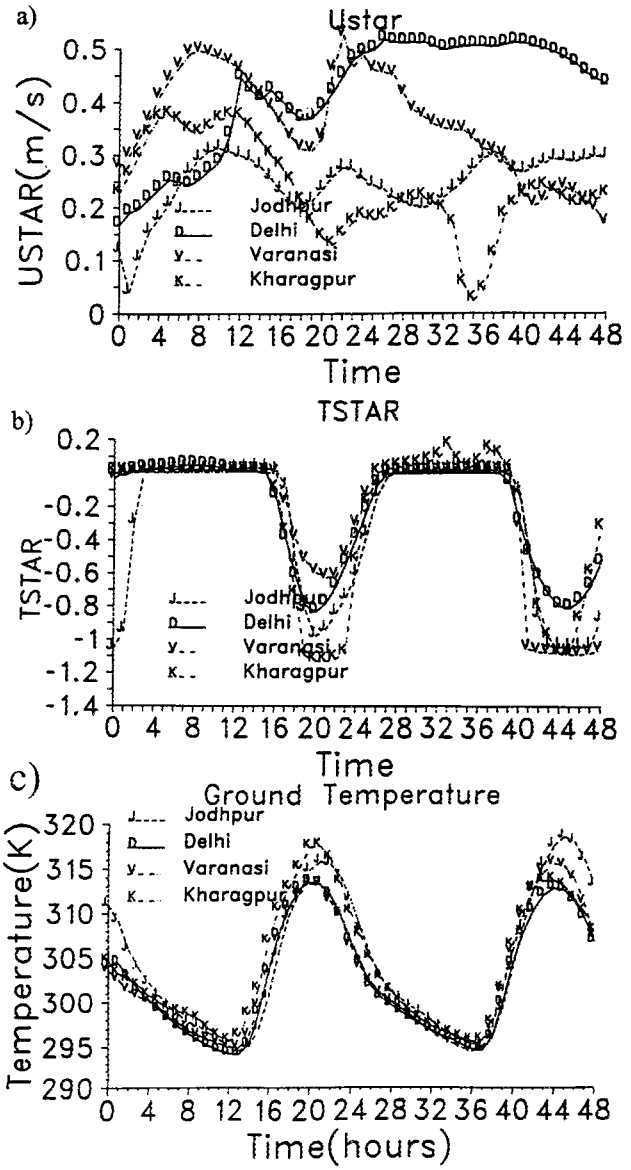

FIG. 6. Diurnal variation of u_*, θ_*, and surface temperature as simulated by the model for the 48 h for various stations. Model integration started at 1730 IST on 3 Aug 1988.

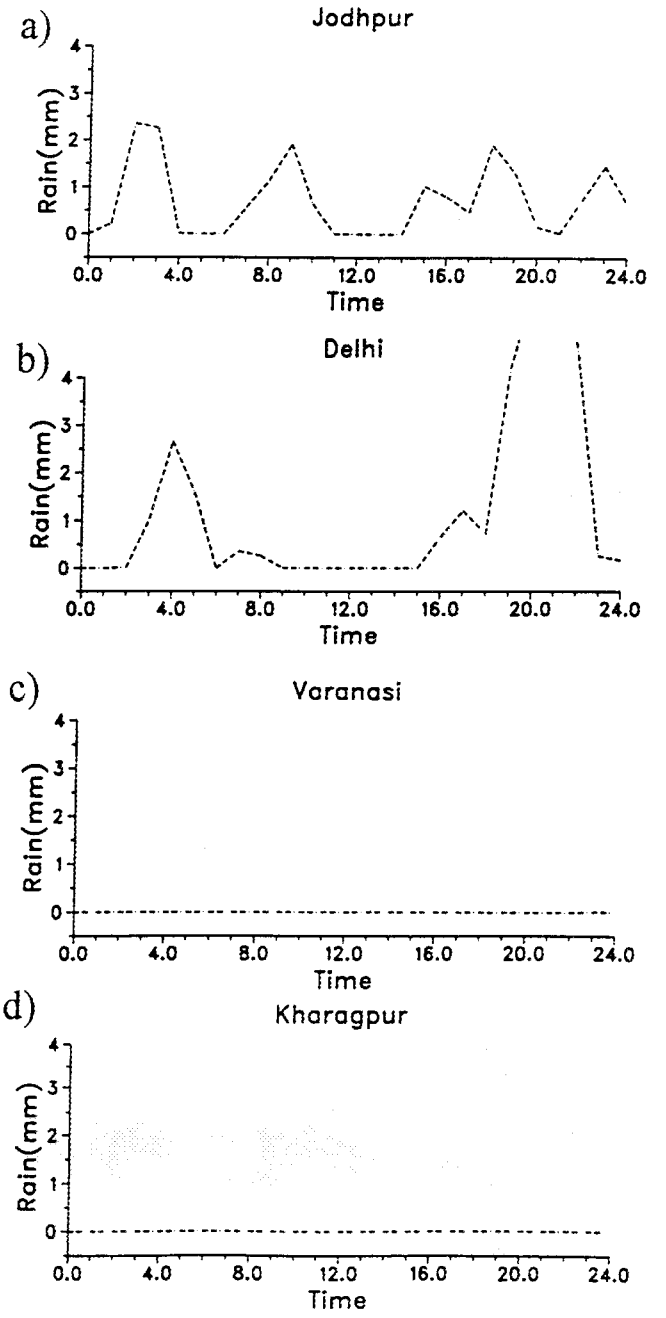

FIG. 7. Hourly accumulated rainfall of first 24 h of model integration at (a) Jodhpur, (b) Delhi, (c) Varanasi, and (d) Kharagpur.

the central part of Madhya Pradesh on 4 August 1988. It further moved in a west-north-westerly direction, intensified into a deep depression, and was located over southeast Rajasthan at 0300 UTC on 5 August. Figure 3 shows the initial analysis of wind fields, temperature, and streamlines at 0.9 σ level and the mean sea level pressure at 1200 UTC on 3 August 1988. Initial analysis shows the presence of the depression, which has already moved onto the land. This feature can be seen in the wind fields and streamlines as well (Figs. 3a,c). The analysis also shows that the depression is well developed on 3 August at 1200 UTC, with a central pressure of 993.2 hPa.

b. *Large-scale fields*

Simulation results of large-scale fields up to 48 h of model integration show that the performance of the model is reasonably good. Figure 4 gives the 48-h forecast of wind at 0.55 and 0.9 σ levels (Figs. 4b,d). Verification analysis of wind for the corresponding levels at 1200 UTC on 5 Aug 1988 is also provided (Figs. 4a,c) for comparison. The model could simulate the vortex of the depression, position, and intensity up to 48

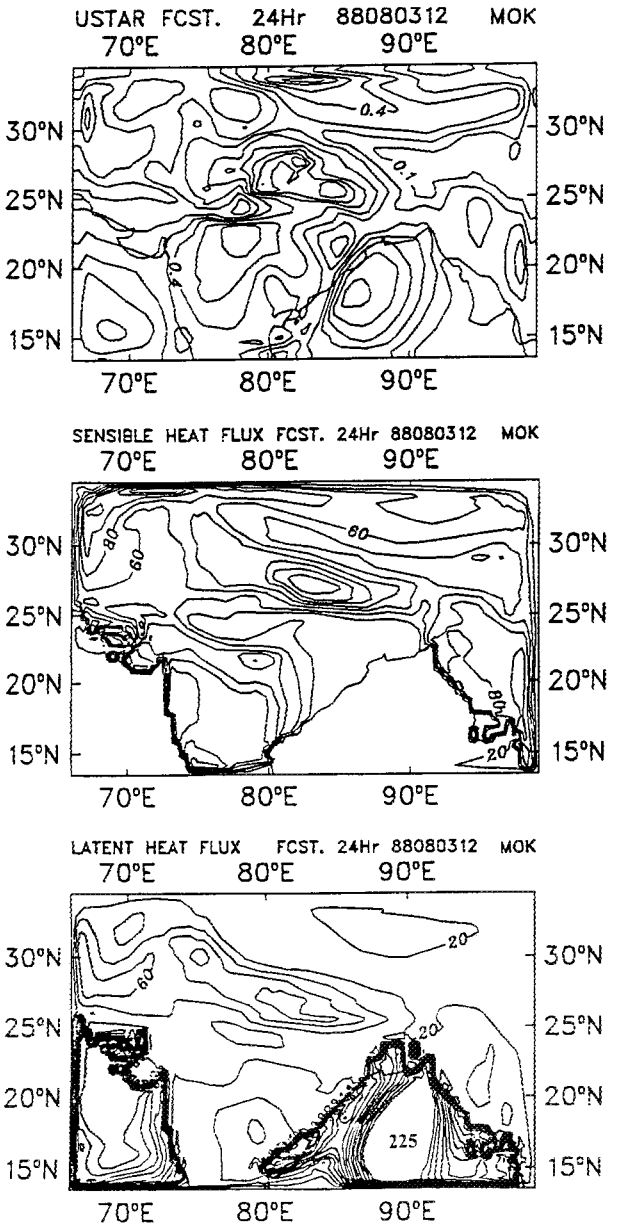

FIG. 8. Model forecast (24 h) of surface parameters (a) friction velocity (m s^{-1}), (b) sensible heat flux (W m^{-2}), and (c) latent heat flux (W m^{-2}).

h with this improved physics for PBL parameterization. The observed feature of maximum wind over the northern quadrant of the depression at lower levels (Rao 1976) have been simulated by the model reasonably well, though the magnitude of the wind speed forecast is slightly more than the corresponding verification analysis at 0.9 σ level. The wind speed at the northern quadrant of the vortex at 0.9 σ level as given by the analysis is 12.2 m s^{-1}, and that given by the forecast is 16.3 m s^{-1}. The forecast center of the depression, as indicated by the isotach of minimum wind speed, is at 25.2°N and 74.5°E, and the depression center, as given by the verification analysis, is at 26°N and 72.5°E, very close to the forecast. Strong westerly wind over the Arabian Sea and Bay of Bengal is a typical feature during the monsoon period, and they are also simulated well by the model. At 0.55 σ level, the intensity of the forecast wind is less as that compared with the analysis around the depression zone. The model could simulate the maximum wind over the northern quadrant of the depression at this level as well. Over the Himalayan region, simulated magnitudes of wind fields are found to be larger than the analysis values. The high orography over the Himalayan region generated some noise as well. Figures 5a and 5b are 0.9 σ level temperature field of the verification analysis and the day-2 forecast, respectively. Isotherms of forecast and analysis show that the model performed reasonably well in forecasting temperature. The predicted temperature over the depression zone is about 296 K, whereas that given by the verification analysis is about 297 K. Over the peninsular Indian region, the difference in temperature is about 1 K. Over the Arabian Sea and Bay of Bengal, the deviation between the forecast and the analysis is less than 1 K. However, over the Himalayan region, the model under predicted the temperature by about 2 K. Mean sea level pressure after 48 h of model integration (Fig. 5d) shows that the depression vortex and its location are very close to that shown in the verification analysis (Fig. 5c). The analyzed mean sea level pressure at the center of the monsoon depression is 993.2 hPa, whereas that predicted by the model at the depression center is 996.5 hPa, a deviation of 3.3 hPa from the analysis. Location of the center of the depression as given by the analysis is at 25.3°N and 72.6°E, and that predicted by the model at the 48th h of model integration is at 25.2°N and 74.3°E, leading to a forecast vector displacement error of about 160 km.

c. *Surface characteristics at specific locations*

Fluxes of heat and momentum at the surface are mainly responsible for the evolution and development of boundary layer over a near homogeneous region. By analyzing the scaling factors of wind (u_*) and temperature (θ_*), one can have a good idea of the development of PBL at the place. Figure 6 shows the diurnal variation of frictional velocity (u_*), scaling temperature (θ_*), and surface temperature simulated at the four stations by the model up to 48 h of integration. Because surface temperature is specified as a surface boundary value over the ocean grid points throughout the model integration, the diurnal variations at oceanic points are not considered. Figure 6a does not show any specific diurnal variation of u_* at any of the stations, and it varies from 0.03 to 0.37 m s^{-1} for Kharagpur, 0.172 to 0.53 m s^{-1} for Delhi, 0.18 to 0.52 m s^{-1} at Varanasi, and 0.04 to 0.31 m s^{-1} at Jodhpur. At the start of the model integration (1200 UTC 3 Aug 1988), the position of the depression is almost equidistant from Kharagpur and

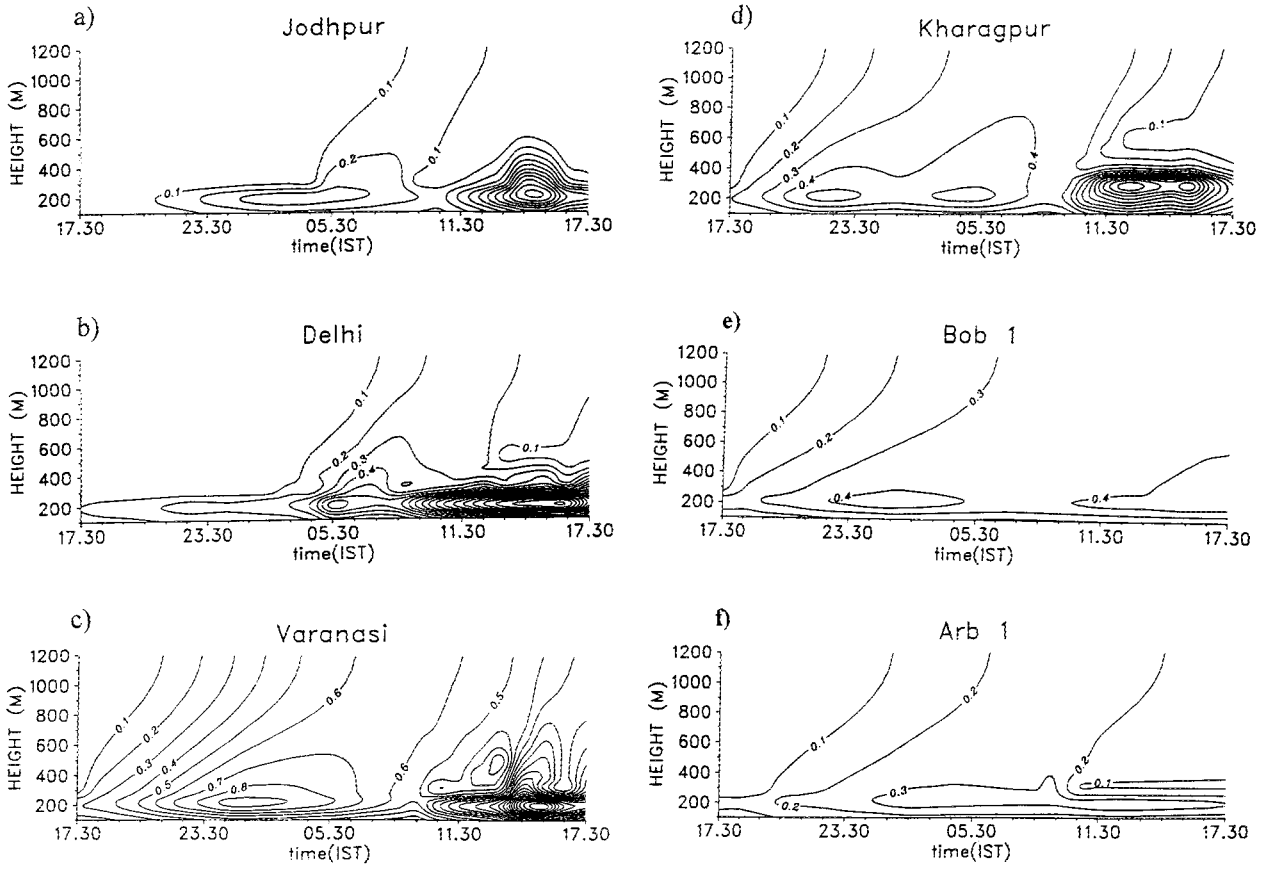

FIG. 9. Diurnal variation of TKE ($m^2 s^{-2}$) with height of first 24 h of integration at (a) Jodhpur, (b) Delhi, (c) Varanasi, (d) Kharagpur, (e) Bay of Bengal, and (f) Arabian Sea.

Varanasi (Fig. 1), and identical values of u_* have been predicted at that time at Kharagpur (0.24 m s^{-1}) and Varanasi (0.27 m s^{-1}). As the depression started moving away from the region, the magnitude of u_* also started falling at Kharagpur except for the initial spinup time. At the same time, the magnitude of u_* started increasing slowly at Varanasi due to the approaching depression. At about the 10th h of model simulation, the frictional velocity attained its peak value of 0.49 m s^{-1} at Varanasi. During the 20th h of integration, frictional velocity has reduced to 0.16 m s^{-1} at Kharagpur and to 0.31 m s^{-1} at Varanasi, and by that time, the simulated depression has already moved away to the central part of the country. The model predicted a low u_* value (0.17 m s^{-1}) at Delhi initially. As the monsoon depression advanced toward northwest direction, magnitude of the predicted u_* at Delhi also increased. During the 24th h of integration, the depression has reached close to Delhi, and u_* also increased to about 0.5 m s^{-1}. From 24 to 48 h of model integration, the distance between the locations of the depression and Delhi was approximately constant, and hence, the magnitude of u_* also maintained about 0.5 m s^{-1}. Based on the MONTBLEX datasets, Mohanty et al. (1995) showed that with the approach of depressions, the frictional velocity increases. The depression did not influence much on u_* at Jodhpur until 32 h of integration, and hence, u_* also maintained a comparatively low magnitude throughout the model integration (0.04 to 0.31 m s^{-1}), though its average value was increasing slowly throughout. The numerical results do not show definite diurnal variation of u_* along the mean monsoon trough due to the passage of depression. However, change in u_* values can be noticed around the depression. Various observational studies over the monsoon trough with the MONTBLEX datasets also showed an increase of u_* with the approach of monsoon depressions (Narasimha et al. 1997).

Figure 6b shows the diurnal variation of θ_* at the 4 land stations for the 48 h of model integration. Unlike u_*, temperature scale θ_* shows a definite diurnal variation over the entire length of the monsoon trough. This figure clearly shows that the instability due to the thermodynamic effect is maximum in the early afternoon. The magnitude of θ_* becomes as low as -1.15 K over Kharagpur at 1330 Indian standard time (IST). The time predicted for minimum θ_* has a phase lag of 1 h between Kharagpur and Jodhpur, with Kharagpur coming first due to the geographical sequence of location of these stations. In Fig. 6c, the model predicted ground temperature for all the four stations are plotted. Comparison

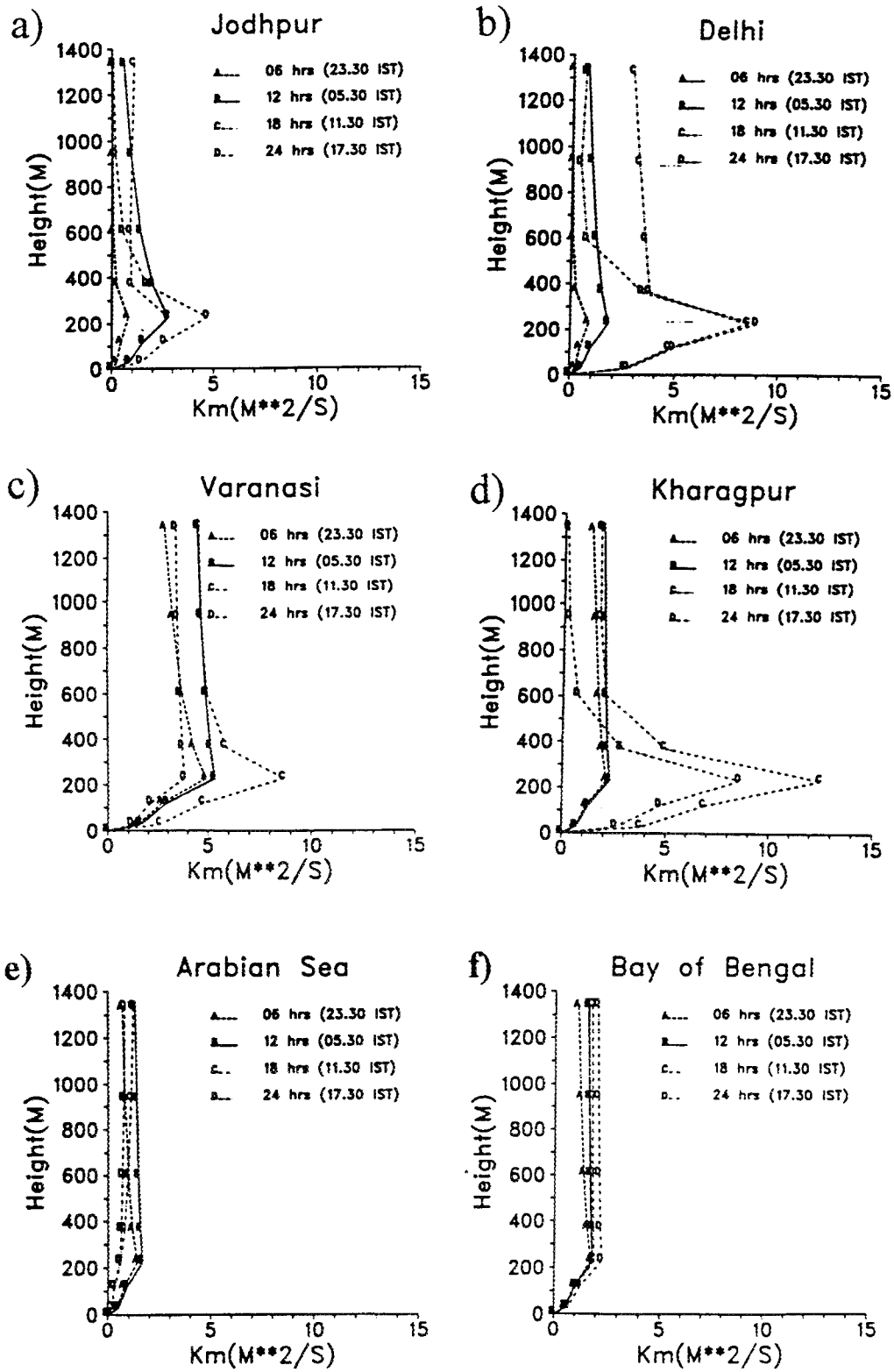

FIG. 10. Vertical profiles of eddy viscosity ($m^2 s^{-1}$) at 6-h interval of model integration at (a) Jodhpur, (b) Delhi, (c) Varanasi, (d) Kharagpur, (e) Arabian Sea, and (f) Bay of Bengal.

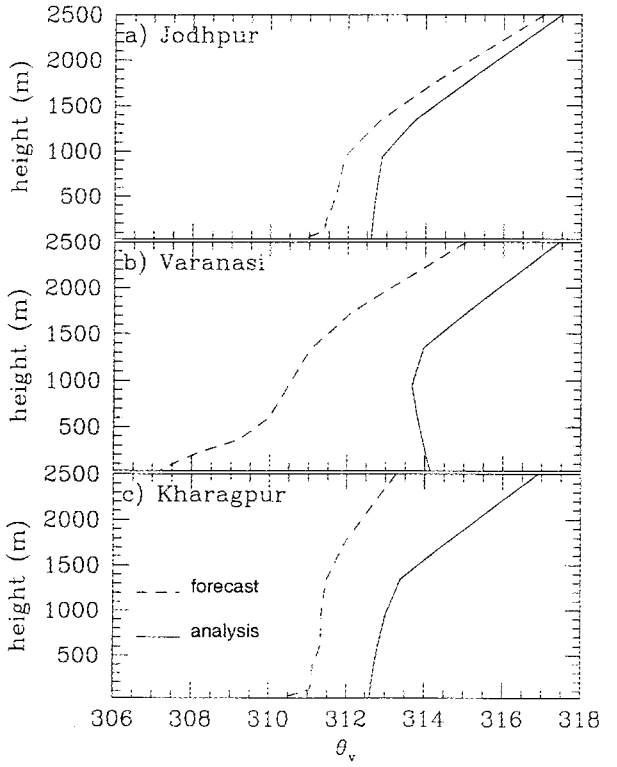

FIG. 11. Observed and predicted virtual potential temperature profile on 4 Aug 1988 at 1200 UTC at (a) Jodhpur, (b) Varanasi, and (c) Kharagpur.

of Fig. 6b and 6c show that the variation of θ_* is in phase with the diurnal variation of ground temperature. Sensible heat flux controls the thermal development of PBL, and given that θ_* is a measure of sensible heat flux, ground temperature at any particular place is the main factor that decides the evolution and development of PBL due to thermal effects. Model-simulated precipitation (accumulated hourly up to 24 h) for all the stations are depicted in Fig. 7. Throughout the model integration, no precipitation occurred over Varanasi and Kharagpur. Because rainfall occurred over Jodhpur and Delhi, the ground temperature could not rise much over Delhi and Jodhpur, though those stations fall in the western end of the monsoon trough. At about 20th h of simulation (1330 IST), a maximum ground temperature of 317.8 K was predicted at Kharagpur, whereas Jodhpur had some rainfall during this time, and hence the ground temperature was less (316 K) as compared with that over Kharagpur. In Delhi, during 1330 IST, about 6 mm of rainfall was received (Fig. 7b), and hence the predicted ground temperature fell as low as 313.2 K. Though Varanasi had no rainfall during the model integration time, the ground temperature failed to go up like in Kharagpur. Cloudiness formed over Varanasi due to the effect of monsoon depression, which might have prevented the increase of ground temperature over there. The forecast of frictional velocity and sensible and latent heat fluxes at the 24th h of model integration are illustrated in Fig. 8. All the panels in the figure (Figs. 8a–c) show sharp gradients at about 26°N and 84°E, which happened to be the location of the storm at that time. The maximum value of u_* went as high as 0.72 m s^{-1} at the southwest quadrant of the depression, where maximum rainfall normally occur. The maximum sensible heat flux predicted around the depression is 142 W m^{-2}, whereas the predicted maximum latent heat flux is 84 W m^{-2} at the depression center. Such sharp contour gradients of fluxes at the storm center suggest low-level convergence around the depression. Because soil moisture was not directly included in the model, surface conditions and the soil wetness were estimated using a climatological albedo factor. Hence, the model results do not reflect the fluxes due to soil moisture conditions during the simulation. An appropriate land surface parameterization may be able to simulate the soil moisture better.

Evolution of PBL at several salient locations of the model domain can be studied by analyzing the variation of TKE as it is considered to be a measure of turbulence intensity. Figure 9 depicts the diurnal variation of TKE with height at every hour of the model integration for 4 land points and 2 oceanic points for the first 24 h of model integration. The figure shows that the evolution of TKE from day to night conditions over the land points is the most dominant feature. No significant variations in the TKE magnitudes are observed over the oceanic points due to the constant surface temperature. Similarly, the vertical extent of TKE is found to be minimum over the sea locations throughout the model integration. Over the land, TKE magnitudes are found to be more during the late afternoon time (1300–1500 IST). The height of the maximum magnitude of TKE is found to be around 200 m in the trough region except over Kharagpur (300 m), which may be due to the high ground temperature. Maximum TKE produced at Jodhpur is 1.1 m^2 s^{-2}, and that simulated by the model at Delhi, Varanasi, and Kharagpur is 2.0, 2.2, and 1.2 m^2 s^{-2}, respectively. These results show that height of maximum TKE is proportional to the ground temperature and not to the magnitude of TKE itself. The highest ground temperature predicted by the model at the 24th h is at Kharagpur, whereas the magnitude of maximum TKE is predicted at Varanasi. Also, the simulation shows that the vertical gradients of TKE with high magnitudes at Delhi, Varanasi, and Jodhpur are consistent with the location of the storm as shown in Fig. 9 and the predicted u_* values in Figs. 6 and 8. The fluxes and the turbulence predicted by the model are influenced by the wind speed. As noted above, for this study, soil wetness is given by the climatological albedo values from a dataset with a resolution of 1° × 1° lat–long, and they do not change during the simulation. Because of the influence of the monsoon depression, a secondary maximum was predicted at Varanasi at 0130 IST (Fig. 9c). A weak

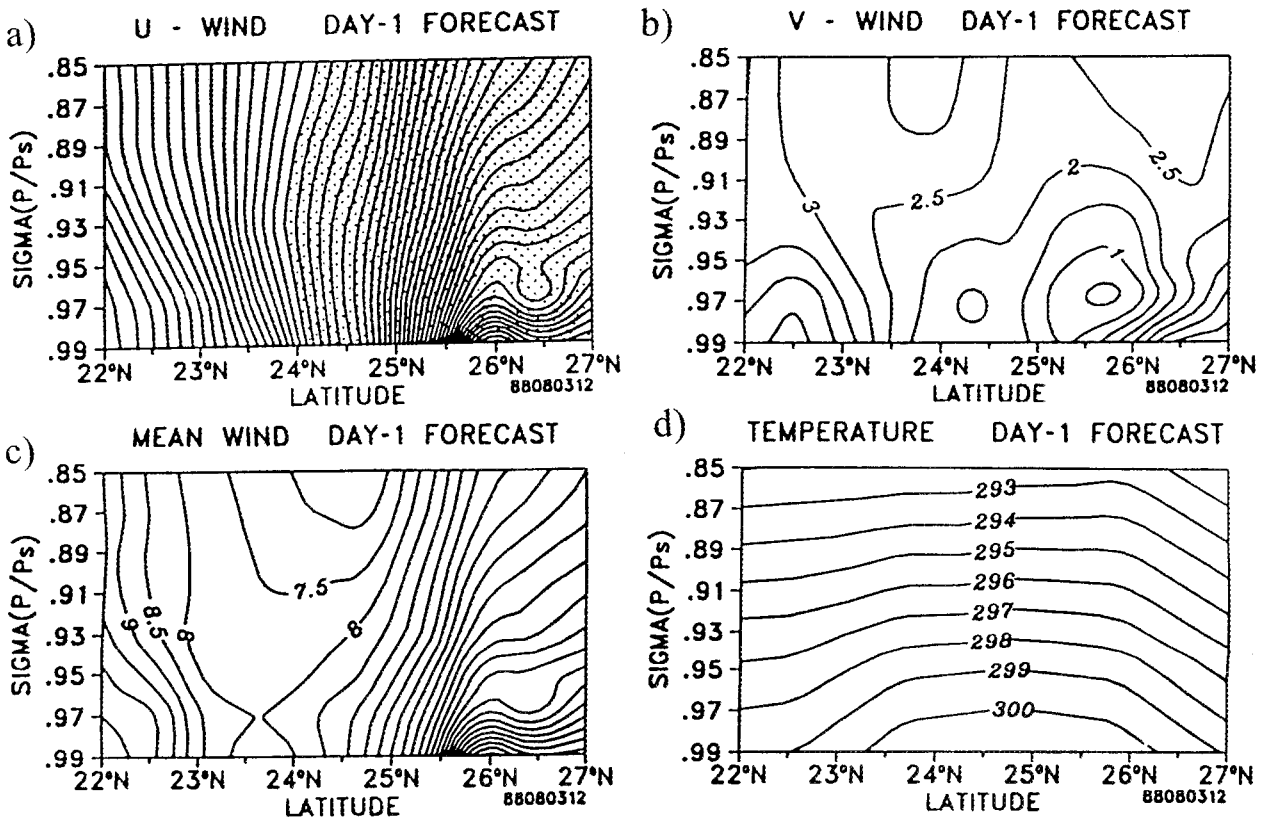

FIG. 12. Zonally averaged fields of wind and temperature with height after 24 h forecast (a) zonal component of wind (stippled area corresponds to easterlies), (b) meridional component of wind, (c) mean wind, and (d) temperature.

secondary maximum can be seen in Delhi at 0530 IST for the same reason.

The vertical profiles of eddy viscosity coefficient (K_m; Fig. 10) depicted at 6-h intervals of the model integration are analyzed to study the evolution of PBL characteristics at various selected points of the domain. Results show that the variation of eddy viscosity with time is marginal over the oceanic points as compared with the land points. Among the land points considered, Kharagpur predicted maximum K_m (13.7 $m^2 s^{-1}$) at 1130 IST. Because of the rainfall and associated phenomena, Jodhpur predicted least K_m (5 $m^2 s^{-1}$). The height of maximum eddy viscosity is found to be more or less the same for all the stations and time. Because the model does not have sufficient vertical resolution at that height, maximum K_m is predicted in the nearest model level, which happens to be same for all the stations.

Observational datasets at selected stations show that the model simulated boundary layer height over the monsoon trough region is in good agreement with the observations. In Fig. 11, vertical profiles of virtual potential temperature at Jodhpur, Varanasi, and Kharagpur are given (solid line). This time corresponds to the 24-h forecast of the model based on the observations on 4 August 1988 at 1200 UTC. The 24-h forecast of virtual potential temperature profiles at the above stations are also given in the figure (dashed lines). From this figure, one can see that mixing is taking place very well over the entire length of the monsoon trough. The capping inversion occurred at 937 m at Jodhpur at the time of observation. The boundary layer height simulated by the model at that time is about 950 m (Fig. 11a). The computed inversion layer of virtual potential temperature at Varanasi based on the observations and model forecast is about 1000 m. Similar boundary layer height of about 1300 m can be estimated for Kharagpur based on the observations as well as the model forecast.

d. Vertical cross sections

The latitudinal and longitudinal mean vertical cross sections of wind and temperature fields is also analyzed over the monsoon trough region to identify the characteristic features of PBL generated by the model physics. A domain of 22°–27°N and 70°–90°E is chosen for averaging, which usually covers the normal monsoon trough region and predominantly covers the land region. Zonal average of vertical cross section of u wind after 24 h of the model integration are shown in Fig. 12a. The dotted area is indicated for negative wind (easterlies). In the figure, calm wind zone (about 24°N) indicates the trough line and has a slope toward the south

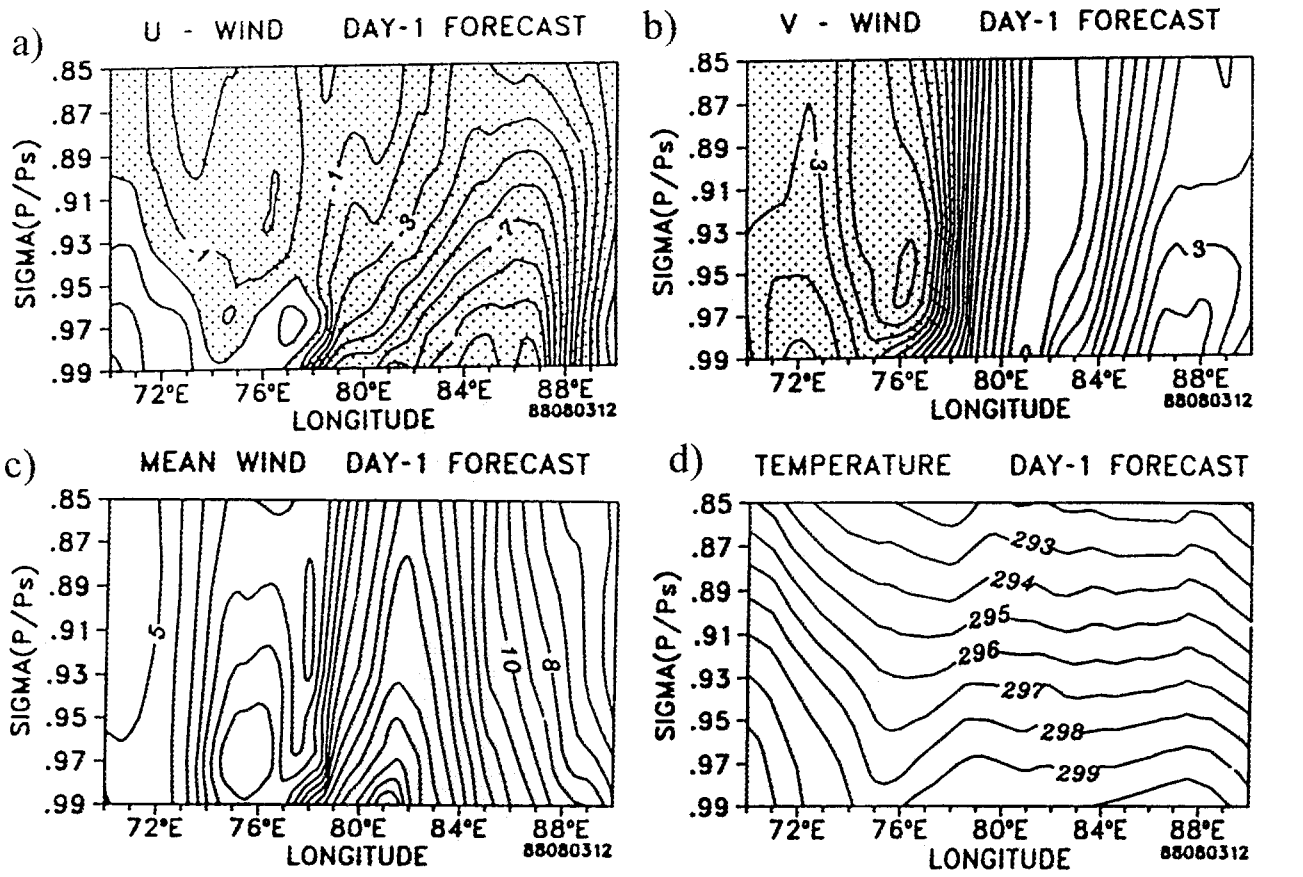

FIG. 13. Same as in Fig. 12 but for meridionally averaged fields of wind and temperature.

with height. Observational studies show that the monsoon trough slopes southward with height, with west-to-southwest winds to the south and easterlies to the north of the trough (Srinivasan et al. 1971). This feature of westerlies to the south and easterlies to the north of the trough line is also simulated reasonably well by the model. Figures 12a–c show the presence of high magnitude of wind, which is one of the characteristics of the monsoon trough boundary layer. Figure 12d depicts the sectorial average of temperature with height. For a particular height, Fig. 12d shows that the temperature at the northern side of the trough is higher than that at the southern side. The air mass to the south of the trough line is coming from the Arabian Sea and is comparatively cool, while the air to the north may have traveled over the Bay of Bengal. Observational studies also show that the air temperature north of the monsoon trough is higher than that at the southern side of the trough (Rao 1976).

Meridional mean of wind and temperature for the 24-h forecast is depicted in Fig. 13. Results show wind with larger magnitude in the lower levels of the model. Observational studies show the presence of low-level wind maxima during the monsoon period (Godbole 1977; Tyagi et al. 1994). Numerical results also show the dominance of westerly winds over the western region of the trough. Observational studies by Rao (1976) show that the western end of the trough is warmer than the eastern side (Fig. 13d).

5. Conclusions

Monsoon trough features, such as southward slope of the trough with height, westerly wind to the south and easterly wind to the north of the trough line, warmer mass over the northern side of the trough line, and so on, are simulated by the regional model based on the TKE closure scheme. The model is able to predict the large-scale fields and the evolution of the PBL structure reasonably well.

The height of PBL increases from the eastern side of the monsoon trough to the western sector because of the dominant thermodynamic effects at the western desert sector. The presence of depression at the eastern side triggers maximum turbulence around the region, resulting in high boundary layer height toward the eastern side of the monsoon trough.

Planetary boundary layer structure over the monsoon trough region based on the simulation results of the regional model shows that in general, along the monsoon trough, the generation of TKE is a marked feature over land as compared with ocean, and its diurnal var-

iation is prominent over the land surface. The maximum magnitude of TKE over the land region of the trough occurs at late afternoon and is on the order of 1–2 $m^2 s^{-2}$. The TKE increases from the eastern end of the monsoon trough to the western side, though with the passage of any systems like monsoon depressions, it is likely to vary. The TKE and its diurnal variation are prominent over the land surface. Higher ground temperature occurs at the western end of the trough as compared with the eastern side, and hence the sensible heat flux will be more over the dry western sector of the monsoon trough. The presence of strong winds in the low levels, which is a characteristic feature of the turbulent monsoon boundary layer, is well simulated by the TKE-based boundary layer physics.

Acknowledgments. The authors are thankful to European Centre for Medium-Range Weather Forecasts for providing the analyzed datasets and National Centre for Medium-Range Weather Forecasting (NCMRWF), New Delhi, India, for extending computer facilities to carry out this study. The U.S. Office of Naval Research supported part of the work. The authors are also grateful to the anonymous referees for giving constructive comments to improve the manuscript substantially.

REFERENCES

Alapaty, K., Sethu Raman, and R. V. Madala, 1994: Simulation of monsoon boundary layer processes using a regional scale nested grid model. *Bound.-Layer Meteor.*, **67,** 407–426.

Arakawa, A., and V. R. Lamb, 1977: *Computational Design of the Basic Dynamical Process of the UCLA General Circulation Model.* Vol. 17, *Methods in Computational Physics,* Academic Press, 173–265.

Businger, J. A., J. C. Wyngaard, Y. Izumi, and E. F. Bradley, 1971: Flux-profile relationships in the atmospheric surface layer. *J. Atmos. Sci.*, **28,** 181–189.

Charnock, H., 1955: Wind stress on a water surface. *Quart. J. Roy. Meteor. Soc.*, **81,** 639–640.

Daly, B. J., and F. H. Harlow, 1970: Transport equations in turbulence. *Phys. Fluids,* **13,** 2634–2649.

Das, N., D. S. Desai, and N. C. Biswas, 1989: Weather of monsoon season (June–September 1988). *Mausam,* **40,** 351–364.

Das, P. K., 1986: Monsoons. Fifth IMO lecture. WMO 613, 155 pp.

Deardorff, J. W., 1974: Three-dimensional numerical study of turbulence in an entraining mixed layer. *Bound.-Layer Meteor.*, **7,** 199–226.

Detering, H. W., and D. Etling, 1985: Application of the E–ϵ turbulence model to the atmospheric boundary layer. *Bound.-Layer Meteor.*, **33,** 113–133.

Godbole, R. V., 1977: The composite structure of the monsoon depression. *Tellus,* **29,** 25–40.

Goel, M., and H. N. Srivasthava, 1990: Monsoon Trough Boundary Layer Experiment (MONTBLEX). *Bull. Amer. Meteor. Soc.*, **71,** 1594–1600.

Holt, T., and Sethu Raman, 1988: A review and comparative evaluation of multilevel boundary layer parameterisations for first-order and turbulent kinetic energy closure schemes. *Rev. Geophys.*, **26,** 761–780.

Krishnamurti, T. N., K. S. Arun Kumar, A. P. Yap, N. D. Dastoor, and J. Sheng, 1990: Performance of a high-resolution mesoscale tropical prediction model. *Advances in Geophysics,* Vol. 32, Academic Press, 133–286.

Kumar, A., 1989: A documentation of the FSU limited area model. Rep. 89-4, Department of Meteorology, The Florida State University, Tallahassee, FL, 301 pp.

Kusuma, G. R., Sethu Raman, and A. Prabhu, 1991: Boundary-layer heights over the monsoon trough region during active and break phases. *Bound.-Layer Meteor.*, **57,** 129–138.

Lazic, L., and B. Talenta, 1990: Documentation of the UB/NMC (University of Belgrade and National Meteorological Centre, Washington) ETA model. Tropical Meteorology Research Programme Rep. 40, WMO/TD 366, 304 pp.

Lykossov, V. N., G. R. Kusuma, and A. Prabhu, 1991: Simulation of the temporal evolution of the atmospheric boundary layer over the monsoon trough region with one-dimensional TKE–dissipation closure model. Centre for Atmospheric Sciences, Indian Institute of Science, Rep. 90 AS3, Bangalore, India, 104 pp.

Madala, R. V., 1978: Efficient time integration schemes for atmosphere and ocean. *Finite Difference Techniques for Vectorized Fluid Dynamics Calculations,* D. L. Book, Ed., Springer-Verlag, 56–74.

——, S. W. Chang, U. C. Mohanty, S. C. Madan, R. K. Paliwal, V. B. Sarin, T. Holt, and Sethu Raman, 1987: Description of Naval Research Laboratory limited area dynamical weather prediction model. NRL Tech. Rep. 5992, 131 pp.

Mailhot, J., and R. Benoit, 1982: A finite element model of the atmospheric boundary layer suitable for use with numerical weather prediction. *J. Atmos. Sci.*, **39,** 2249–2266.

Mohanty, U. C., R. K. Paliwal, and A. Tyagi, 1990: Application of split-explicit time integration scheme to a multi-level limited area model and forecast performance over Indian region. *Mausam,* **41,** 531–540.

——, ——, T. Venugopal, and Parashuram, 1995: Estimation of drag coefficient over the western desert sector of the Indian Summer monsoon trough. *Proc. Indian Acad. Sci. Earth Planet. Sci.*, **104,** 157–187.

Monin, A. S., and A. M. Yaglom, 1971: *Statistical Fluid Mechanics.* Vol. 1. MIT Press, 468–504.

Narasimha, R., D. R. Sikka, and A. Prabhu, 1997: *The Monsoon Trough Boundary Layer.* Indian Academy of Sciences, 422 pp.

Perkey, D. J., and C. W. Kreitzberg, 1976: A time dependent lateral boundary scheme for limited area primitive equation models. *Mon. Wea. Rev.*, **104,** 744–755.

Potty, K. V. J., U. C. Mohanty, and S. Raman, 1997: Effect of three different boundary-layer parameterisations in a regional atmospheric model on the simulation of summer monsoon circulation. *Bound.-Layer Meteor.*, **84,** 363–381.

Rao, Y. P., 1976: Southwest monsoon. *Synoptic Meteorology, Meteor. Monogr.*, No. 1/7, India Meteorological Department, 107–185.

Sikka, D. R., and R. Narasimha, 1995: Genesis of the Monsoon Trough Boundary Layer Experiment (MONTBLEX). *Proc. Indian Acad. Sci. Earth Planet. Sci.*, **104,** 157–187.

Srinivasan, V., S. Raman, and S. Mukherji, 1971: Southwest monsoon—typical situations over Madhya Pradesh and Vidarbha. India Meteorological Department, FMU Rep. III-3.4, 12–21.

Tyagi, A., U. C. Mohanty, and K. J. Ramesh, 1994: Planetary boundary layer structure in the monsoon trough region. *Mausam,* **45,** 213–222.

Wyngaard, J. C., 1975: Modeling the planetary boundary layer—extension to the stable case. *Bound.-Layer Meteor.*, **9,** 441–460.